

## Article

# Thermoresponsive Property of Poly(*N,N*-bis(2-methoxyethyl)acrylamide) and Its Copolymers with Water-Soluble Poly(*N,N*-disubstituted acrylamide) Prepared Using Hydrosilylation-Promoted Group Transfer Polymerization

Xiangming Fu <sup>1</sup>, Yanqiu Wang <sup>1</sup>, Liang Xu <sup>1</sup>, Atsushi Narumi <sup>2</sup> , Shin-ichiro Sato <sup>3</sup>, Xiaoran Yang <sup>1</sup>, Xiande Shen <sup>1,4,\*</sup> and Toyoji Kakuchi <sup>1,3,4,\*</sup> 

<sup>1</sup> Research Center for Polymer Materials, School of Materials Science and Engineering, Changchun University of Science and Technology, Weixing Road 7989, Changchun 130022, China; 18846321589@163.com (X.F.); yqwang@cust.edu.cn (Y.W.); m13069984921@163.com (L.X.); 18686350018@163.com (X.Y.)

<sup>2</sup> Graduate School of Organic Materials Science, Yamagata University, 4-3-16 Jonan, Yonezawa 992-8510, Yamagata, Japan; narumi@yz.yamagata-u.ac.jp

<sup>3</sup> Division of Applied Chemistry, Faculty of Engineering, Hokkaido University, Sapporo 060-8628, Hokkaido, Japan; s-sato@eng.hokudai.ac.jp

<sup>4</sup> Chongqing Research Institute, Changchun University of Science and Technology, No. 618 Liangjiang Avenue, Longxing Town, Yubei District, Chongqing 401135, China

\* Correspondence: shenxiande@cust.edu.cn (X.S.); kakuchi@eng.hokudai.ac.jp (T.K.)



**Citation:** Fu, X.; Wang, Y.; Xu, L.; Narumi, A.; Sato, S.-i.; Yang, X.; Shen, X.; Kakuchi, T. Thermoresponsive Property of Poly(*N,N*-bis(2-methoxyethyl)acrylamide) and Its Copolymers with Water-Soluble Poly(*N,N*-disubstituted acrylamide) Prepared Using Hydrosilylation-Promoted Group Transfer Polymerization. *Polymers* **2023**, *15*, 4681. <https://doi.org/10.3390/polym15244681>

Academic Editors: Dimitrios Bikiaris, Asterios (Stergios) Pispas, Ian Wyman, Athanasios Skandalis and Theodore Sentoukas

Received: 3 November 2023

Revised: 5 December 2023

Accepted: 9 December 2023

Published: 12 December 2023



**Copyright:** © 2023 by the authors. Licensee MDPI, Basel, Switzerland. This article is an open access article distributed under the terms and conditions of the Creative Commons Attribution (CC BY) license (<https://creativecommons.org/licenses/by/4.0/>).

**Abstract:** The group-transfer polymerization (GTP) of *N,N*-bis(2-methoxyethyl)acrylamide (MOEAm) initiated by Me<sub>2</sub>EtSiH in the hydrosilylation-promoted method and by silylketene acetal (SKA) in the conventional method proceeded in a controlled/living manner to provide poly(*N,N*-bis(2-methoxyethyl)acrylamide) (PMOEAm) and PMOEAm with the SKA residue at the  $\alpha$ -chain end (MCIP-PMOEAm), respectively. PMOEAm-*b*-poly(*N,N*-dimethylacrylamide) (PDMAm) and PMOEAm-*s*-PDMAm and PMOEAm-*b*-poly(*N,N*-bis(2-ethoxyethyl)acrylamide) (PEOEAm) and PMOEAm-*s*-PEOEAm were synthesized by the block and random group-transfer copolymerization of MOEAm and *N,N*-dimethylacrylamide or *N,N*-bis(2-ethoxyethyl)acrylamide. The homo- and copolymer structures affected the thermoresponsive properties; the cloud point temperature ( $T_{cp}$ ) increasing by decreasing the degree of polymerization ( $x$ ). The chain-end group in PMOEAm affected the  $T_{cp}$  with PMOEAm <sub>$x$</sub>  > MCIP-PMOEAm <sub>$x$</sub> . The  $T_{cp}$  of statistical copolymers was higher than that of block copolymers, with PMOEAm <sub>$x$</sub> -*s*-PDMAm <sub>$y$</sub>  > PMOEAm <sub>$x$</sub> -*b*-PDMAm <sub>$y$</sub>  and PMOEAm <sub>$x$</sub> -*s*-PEOEAm <sub>$y$</sub>  > PMOEAm <sub>$x$</sub> -*b*-PEOEAm <sub>$y$</sub> .

**Keywords:** poly(*N,N*-bis(2-methoxyethyl)acrylamide); thermoresponsive property; cloud point temperature; group transfer polymerization; hydrosilylation-promoted GTP

## 1. Introduction

Thermoresponsive polymers exhibit a reversible phase transition in response to a change in temperature. The most common thermoresponsive polymers are those with lower critical solution temperatures, which are soluble in a particular solvent at low temperatures but insoluble at high temperatures [1–5], such as poly(*N*-isopropylacrylamide) (PNIPAm) [6–9], poly(ethylene glycol) [10–12], poly(2-hydroxyethyl methacrylate) [13–15], poly(methacrylic acid) [16–18], poly(styrene sulfonate) [19,20], poly(vinyl alcohol) [21–23], poly(*N*-vinylcaprolactam) [24–26], and poly(*N,N*-diethylacrylamide) (PDEAm) [27,28]. For example, PNIPAm is soluble in water at room temperature but becomes insoluble in water at body temperature, which renders it suitable for drug delivery, tissue engineering, biosensing, self-assembly, and other uses [29]. Furthermore, the sol-gel conversion of polyacrylamide in water is widely used in applications such as drilling, acidification, water purification, and flocculation [30].

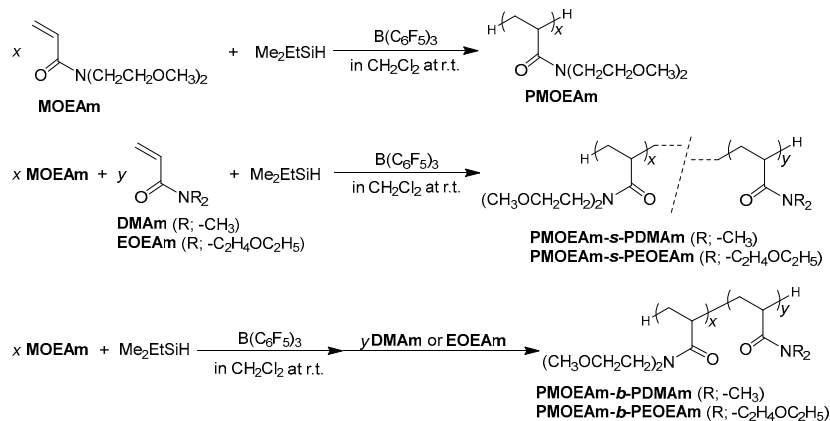
Thus, the development of new thermoresponsive polymers is important to realize new applications. In polymer design, we need to consider that the thermoresponsive property is closely related to the polymer structure, including the primary structure of the polymer main and side chains [31], polymer stereoregularity [32], molecular mass and polydispersity [33], polymer end groups [34], and type of structure, i.e., block [35–38], graft [39–41], cyclic hyperbranched [42,43], and star-shaped [44,45]. To precisely synthesize these polymers, living radical polymerization methods [46], such as nitroxide-mediated polymerization [47,48], atom transfer radical polymerization [49–51], and reversible addition/fragmentation chain transfer (RAFT) polymerization [52–54], are widely used. In these polymerization methods, end groups derived from polymerization initiators are inevitably introduced into the resulting polymers. Since the end groups of polymers affect the thermoresponsive properties, these synthetic methods are not suitable for the characterization of new thermoresponsive polymers in terms of, for example, the molecular mass dependence of the thermoresponsive properties.

Group-transfer polymerization (GTP) is a reliable living polymerization method for polar monomers such as (meth)acrylate, which can be performed using conventional catalysts to produce well-defined polymers [55]. For instance, Taton et al., Waymouth et al., and our group reported that organocatalysts could effectively promote the controlled/living GTP of (meth)acrylate [56,57], alkyl sorbate [58], alkyl crotonate [59], methacrylonitrile [60], and *N,N*-disubstituted acrylamide (DSAm) [61]. These conventional GTP systems require the use of silyl ketene acetal (SKA) or silyl ketene aminal (SKAm) as an initiator, resulting in the attachment of residual groups derived from SKA or SKAm at the  $\alpha$ -chain end of the obtained polymers. Recently, we developed a new GTP method that does not require adding SKA or SKAm beforehand, i.e., the polymerization of (meth)acrylate and acrylamide monomers with hydrosilane ( $R_3SiH$ ) using tris(pentafluorophenyl)borane ( $B(C_6F_5)_3$ ) as the catalyst, which proceeded through a controlled/living GTP mechanism to produce well-defined polymers without  $\alpha$ -chain-end groups derived from SKA or SKAm [62,63]. In this GTP method, SKA or SKAm was formed via the  $B(C_6F_5)_3$ -catalyzed hydrosilylation of a monomer and  $R_3SiH$  in the polymerization system prior to the polymerization. We applied the hydrosilylation-promoted GTP method to the synthesis of thermoresponsive polymers capped with hydrogen atoms in both chain ends, such as PDEAm and poly(*N*-methyl,*N*-*n*-propylacrylamide) [64].

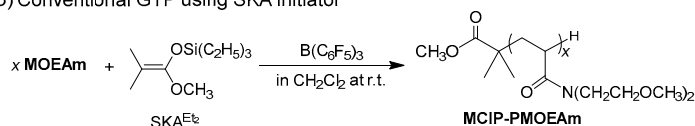
Poly(*N,N*-bis(2-methoxyethyl)acrylamide) (PMOEAm) has been synthesized using radical polymerization methods as a thermoresponsive poly(*N,N*-disubstituted acrylamide). For example, conventional radical polymerization was used for the preparation of PMOEAm [65], PMOEAm-*s*-PNIPAm [66,67], and carboxy-terminated PMOEAm [68], while RAFT polymerization was adopted to produce PMOEAm [69] and PMOEAm-*b*-poly(*N,N*-dimethylacrylamide) (PDMAm) [70], whose  $\alpha,\omega$ -ends were capped with residues derived from the RAFT agent. In addition, we reported that the conventional GTP of *N,N*-bis(2-methoxyethyl)acrylamide (MOEAm) with SKA using an organocatalyst produced PMOEAm functionalized with the SKA residue at the  $\alpha$ -chain end ((methoxycarbonyl)isopropyl (MCIP)-PMOEAm, Scheme 1b). Thus, toward the design and synthesis of thermoresponsive materials consisting of PMOEAm, clarifying the thermoresponsive property of PMOEAm without the influence of terminal groups is important. Here, we report the synthesis of PMOEAm capped with hydrogen atoms at both chain ends via the hydrosilylation-promoted GTP of MOEAm with dimethylethylsilane ( $Me_2EtSiH$ ) using  $B(C_6F_5)_3$  as a catalyst. To broaden the thermoresponsive range of PMOEAm, we synthesized statistical and block copolymers of PMOEAm with water-soluble PDMAm (nonthermoresponsive), and thermoresponsive poly(*N,N*-bis(2-ethoxyethyl)acrylamide) (PEOEAm), utilizing hydrosilylation-promoted group-transfer copolymerization (GTcoP), as displayed in Scheme 1a [71] (Scheme 1a). The effects of differences in the polymer structures between PMOEAm and MCIP-PMOEAm, PMOEAm-*b*-PDMAm and PMOEAm-*s*-PDMAm, and PMOEAm-*b*-PEOEAm and PMOEAm-*s*-PEOEAm on the thermoresponsive behavior were investigated by measuring the nuclear magnetic resonance (NMR) spectra

and dynamic light scattering (DLS) of these polymer solutions before and after the cloud point temperature ( $T_{cp}$ ).

a) Hydrosilylation-promoted GTP using  $R_3SiH$



b) Conventional GTP using SKA initiator



**Scheme 1.** (a) Synthesis of PMOEAm, PMOEAm-*b*-PDMAm and PMOEAm-*s*-PDMAm, and PMOEAm-*b*-PEOEAm and PMOEAm-*s*-PEOEAm via hydrosilylation-promoted group-transfer polymerization (GTP) and (b) synthesis of PMOEAm functionalized with a (methoxycarbonyl)isopropyl (MCIP) group at the  $\alpha$ -chain end (MCIP-PMOEAm) via conventional GTP using silylketene acetal (SKA) as an initiator.

## 2. Materials and Methods

### 2.1. Materials

Dichloromethane ( $CH_2Cl_2$ , >99.5%; water content < 0.001%), methyl alcohol (MeOH), and calcium hydride ( $CaH_2$ ) were purchased from Kanto Chemicals Co., Inc. (Tokyo, Japan). Bis(2-methoxyethyl)amine, DMAm, and  $Me_2EtSiH$  were obtained from Tokyo Kasei Kogyo Co., Ltd. (Tokyo, Japan).  $B(C_6F_5)_3$  was procured from Wako Pure Chemical Industries, Ltd. (Tokyo, Japan) and utilized after recrystallization from *n*-hexane at  $-30$  °C. DMAm and  $CH_2Cl_2$  were distilled using  $CaH_2$  and degassed through three freeze-pump-thaw cycles before being stored under an Ar atmosphere for future use. All other chemicals were purchased from suppliers and used without purification. Polymerizations were carried out in a glove box under Ar atmosphere at 25 °C.

### 2.2. Measurements

$^1H$  NMR spectra were obtained using a Bruker Avance III HD 500 spectrometer from Bruker Corporation (Billerica, MA, USA). Polymerization solutions were prepared in a Mikrouna glove box with a gas purification system consisting of molecular sieves and a copper catalyst and were filled with a dry Ar atmosphere (with  $H_2O$  and  $O_2$  contents of less than 1 ppm). The water and oxygen levels inside the glove box were monitored using the MK-XTR-100 and MK-OX-SEN-1 sensors from Mikarona Industrial Intelligent Technology Co., Ltd. (Shanghai, China), respectively. The polymers' number-average molecular mass ( $M_{n,SEC}$ ) and polydispersity index ( $\mathcal{D}$ ) were measured through size exclusion chromatography (SEC) at 40 °C. The Agilent high-performance liquid chromatography system (1260 Infinity II) was utilized in *N,N*-dimethylformamide (DMF) containing 0.01% lithium chloride. A solution of 1.0 mol  $L^{-1}$  was flowed through Agilent Polar Gel-M columns (exclusion limit,  $2 \times 10^4$  g  $mol^{-1}$ ) and Polar Gel-M columns (exclusion limit,  $4 \times 10^6$  g  $mol^{-1}$ ) ( $7.5 \times 300$  mm; average bead size, 5  $\mu m$ ) (Agilent Technologies Inc. Shanghai, China) at a rate of 1.0 mL  $min^{-1}$ . Cloud-point measurements were taken on a Jasco

V-770 ultraviolet–visible (UV–vis) spectrophotometer (Tokyo, Japan), which was equipped with a Jasco CTU-100 temperature controller. The temperature was then increased at a rate of  $1\text{ }^{\circ}\text{C min}^{-1}$  while the path length was 10 mm. Changes in transmission were recorded at 500 nm with varying temperatures. The hydrodynamic radius ( $R_h$ ) of the produced polymers was analyzed through a Dyna Pro Nanostar<sup>®</sup> instrument from Wyatt Technology in Santa Barbara, CA, USA.

### 2.3. Synthesis of PMOEAm

A solution of MOEAm (749.0 mg, 4 mmol),  $\text{Me}_2\text{EtSiH}$  (5.28  $\mu\text{L}$ , 40  $\mu\text{mol}$ ), and  $\text{B}(\text{C}_6\text{F}_5)_3$  (2.1 mg, 4.0  $\mu\text{mol}$ ) in  $\text{CH}_2\text{Cl}_2$  (3.96 mL) was stirred for 12 h at room temperature in a glove box under an Ar atmosphere. To terminate the polymerization, a small amount of MeOH was added, and then the crude product was purified by dialysis against acetone to obtain a white solid product. The yield was 408.7 mg (54.6%).

### 2.4. Synthesis of MCIP-PMOEAm

A solution of MOEAm (749.0 mg, 4 mmol), 1-methoxy-1-(triethylsiloxy)-2-methyl-1-propene ( $\text{SKA}^{\text{Et}}$ ; 8.64 mg, 40  $\mu\text{mol}$ ), and  $\text{B}(\text{C}_6\text{F}_5)_3$  (2.1 mg, 4.0  $\mu\text{mol}$ ) in  $\text{CH}_2\text{Cl}_2$  (3.96 mL) was stirred for 8 h at room temperature in a glove box under an Ar atmosphere. To terminate the polymerization, a small amount of MeOH was added, and then the crude product was purified by dialysis against acetone to obtain a white solid product. The yield was 408.7 mg (55%).

### 2.5. Synthesis of PMOEAm-s-PDMAm

A solution containing MOEAm (375.5 mg, 2 mmol), DMAm (198.4 mg, 2 mmol),  $\text{Me}_2\text{EtSiH}$  (5.28  $\mu\text{L}$ , 40  $\mu\text{mol}$ ), and  $\text{B}(\text{C}_6\text{F}_5)_3$  (2.1 mg, 4.0  $\mu\text{mol}$ ) in  $\text{CH}_2\text{Cl}_2$  (3.96 mL) was stirred for 12 h at room temperature in a glove box under an Ar atmosphere. To terminate the polymerization, a small amount of MeOH was added, and the crude product was then purified by dialysis against acetone to obtain a white solid product. The yield was 369.1 mg (50%).

### 2.6. Synthesis of PMOEAm-b-PDMAm

A solution containing MOEAm (375.5 mg, 2 mmol),  $\text{Me}_2\text{EtSiH}$  (5.28  $\mu\text{L}$ , 40  $\mu\text{mol}$ ), and  $\text{B}(\text{C}_6\text{F}_5)_3$  (2.1 mg, 4.0  $\mu\text{mol}$ ) in  $\text{CH}_2\text{Cl}_2$  (3.96 mL) was stirred under an Ar atmosphere at room temperature in a glove box for 12 h. A sample of the reaction solution was taken to confirm the complete MOEAm consumption via  $^1\text{H}$  NMR spectroscopy. Afterward, DMAm (198.4 mg, 2 mmol) was introduced to the polymerization mixture and stirred for 36 h. The crude product was then purified following the same procedure used in the synthesis of PEOEAm. The result was a white solid polymer with a yield of 345.9 mg (47%).

## 3. Results and Discussion

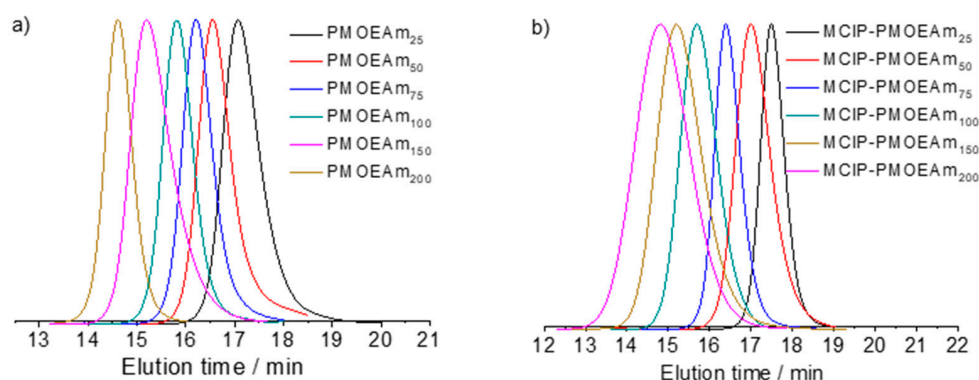
### 3.1. Synthesis of PMOEAm

We reported preliminary results for the GTP of MOEAm with  $\text{SKA}^{\text{Et}}$  or  $\text{Me}_2\text{EtSiH}$  using  $\text{B}(\text{C}_6\text{F}_5)_3$  as the catalyst, i.e., the conventional and hydrosilylation-promoted methods, respectively [72]. In order to clarify the effect of the chain end group, it is necessary to use polymers synthesized under similar polymerization conditions for both GTPs. For the hydrosilylation-promoted GTP of MOEAm with  $\text{Me}_2\text{EtSiH}$ , the polymerization was performed at a  $[\text{MOEAm}]_0/[\text{Me}_2\text{EtSiH}]_0/[\text{B}(\text{C}_6\text{F}_5)_3]_0$  ratio of 25/1/0.1. The  $M_{n,\text{SEC}}$  of the obtained polymer was  $4.5\text{ kg mol}^{-1}$ , which was in good agreement with the calculated molecular mass ( $M_{n,\text{calcd}}$ ) of  $4.7\text{ kg mol}^{-1}$  (Table 1, run 1). The polydispersity index ( $\text{Đ}$ ) of the obtained polymer was as low as 1.13 (Figure 1a). Similarly, the conventional GTP of MOEAm was performed at a  $[\text{MOEAm}]_0/[\text{SKA}^{\text{Et}}]_0/[\text{B}(\text{C}_6\text{F}_5)_3]_0$  ratio of 25/1/0.1 to obtain a polymer with a  $M_{n,\text{SEC}}$  of  $5.1\text{ kg mol}^{-1}$ , which was close to the  $M_{n,\text{calcd}}$  of  $4.9\text{ kg mol}^{-1}$  (Table S1). The SEC trace of the resulting polymer was unimodal with a low  $\text{Đ}$  of 1.11 (Figure 1b).

**Table 1.** Synthesis of poly(*N,N*-bis(2-methoxyethyl)acrylamide) via the hydrosilylation-promoted GTP of MOEAm with Me<sub>2</sub>EtSiH using B(C<sub>6</sub>F<sub>5</sub>)<sub>3</sub> as the catalyst. <sup>a</sup>

Run	Polymer	[MOEAm] <sub>0</sub> /[Me <sub>2</sub> EtSiH] <sub>0</sub> /[B(C <sub>6</sub> F <sub>5</sub> ) <sub>3</sub> ] <sub>0</sub>	Time h	<i>M</i> <sub>n,calcd</sub> <sup>b</sup> kg mol <sup>-1</sup>	<i>M</i> <sub>n,SEC</sub> (Đ) <sup>c</sup> kg mol <sup>-1</sup>	<i>T</i> <sub>cp</sub> <sup>d</sup> °C
1	PMOEAm <sub>25</sub>	25/1/0.1	6	4.7	4.5 (1.13)	56.5
2	PMOEAm <sub>50</sub>	50/1/0.1	6	9.4	9.6 (1.16)	53.9
3	PMOEAm <sub>75</sub>	75/1/0.1	12	14.0	13.8 (1.12)	51.2
4	PMOEAm <sub>100</sub>	100/1/0.1	12	18.7	19.0 (1.11)	50.9
5	PMOEAm <sub>150</sub>	150/1/0.2	12	28.1	28.1 (1.12)	50.5
6	PMOEAm <sub>200</sub>	200/1/0.2	18	37.4	37.1 (1.17)	48.0

<sup>a</sup> [MOEAm] concentration of 1.0 mol L<sup>-1</sup> was used in CH<sub>2</sub>Cl<sub>2</sub> solvent at 25 °C under an Ar atmosphere. Monomer conversion was determined to be >99.9% by <sup>1</sup>H NMR in CDCl<sub>3</sub>. <sup>b</sup> The molecular mass of the polymers was calculated using the equation [MOEAm]/[Me<sub>2</sub>EtSiH]<sub>0</sub> × (conv.) × (M.W. of monomer) + (M.W. of H) × 2. <sup>c</sup> The molecular mass of polymer was determined by SEC equipped with an RI detector in DMF containing lithium chloride (0.01 mol L<sup>-1</sup>) using PMMA as standards. <sup>d</sup> The *T*<sub>cp</sub>s of [MOEAm] was determined by UV-vis measurements in water at 10 g L<sup>-1</sup>.

**Figure 1.** SEC traces of (a) PMOEAm and (b) MCIP-PMOEAm (eluent, DMF containing lithium chloride (0.01 mol L<sup>-1</sup>); flow rate, 1.0 mL min<sup>-1</sup>).

The <sup>1</sup>H NMR spectra of the polymers obtained using the two initiation methods were almost identical, showing signals due to the –NCH<sub>2</sub>CH<sub>2</sub>O–, –OCH<sub>3</sub>, –CH<sub>2</sub>CH–, and –CH<sub>2</sub>CH– groups at 3.83–3.88, 3.31–3.38, 0.99–2.01, and 2.45–2.75 ppm, respectively. In addition, signals due to the –C(CH<sub>3</sub>)<sub>2</sub> group as a residue of SKA<sup>Et</sup> were observed at 1.26 ppm for the polymer prepared using the conventional initiation method (Figure 2). More detailed information on the resulting polymer structures was obtained via matrix-assisted laser desorption/ionization time-of-flight mass spectrometry (MALDI-TOF MS) measurements.

The MALDI-TOF MS spectrum depicted in Figure 3a reveals a sole set of molecular ion peaks with an adjacent peak distance of 187.24 Da, consistent with the molecular mass prediction of MOEAm as the constitutional repeat unit. Moreover, the *m/z* values of each molecular ion peak were in accordance with the sodium-cationized polymer composition of [H-MOEAm<sub>n</sub>-H + Na]<sup>+</sup> (molecular formula: C<sub>9n</sub>H<sub>17n</sub> + <sub>2</sub>H<sub>2</sub>NnO<sub>3n</sub>Na). For example, an *m/z* value of 4705.82 Da corresponds to a sodium-cationized 25-unit polymer structure of [H-MOEAm<sub>25</sub>-H + Na]<sup>+</sup>, with a theoretical monoisotopic value of 4705.03 Da for the molecular formula C<sub>225</sub>H<sub>427</sub>N<sub>25</sub>O<sub>75</sub>Na.

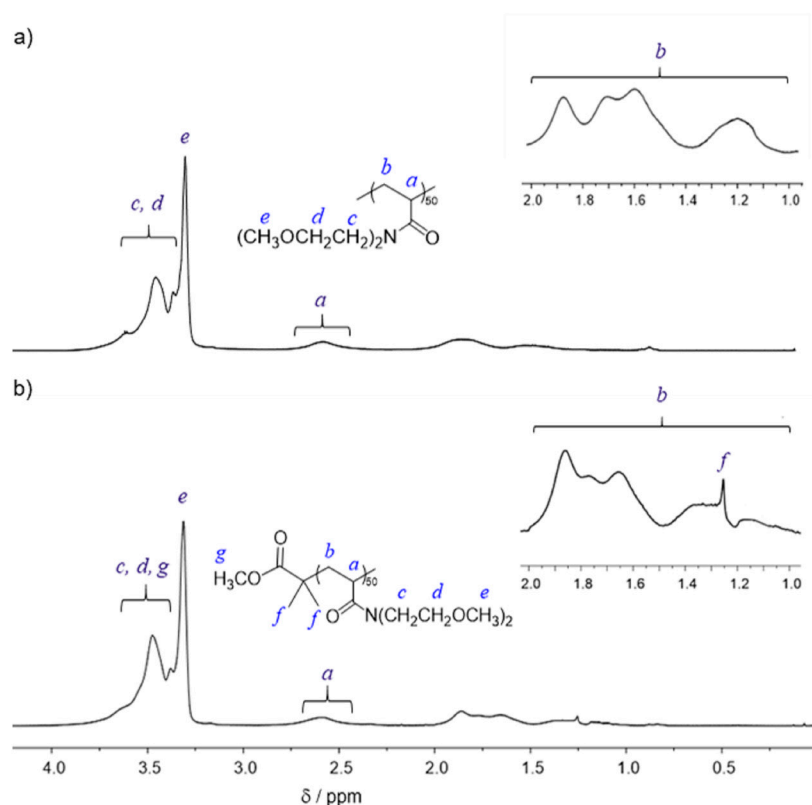


**Figure 2.**  $^1\text{H}$  NMR spectra of (a) PMOEAm<sub>25</sub> and (b) MCIP-PMOEAm<sub>25</sub> in  $\text{CDCl}_3$ .

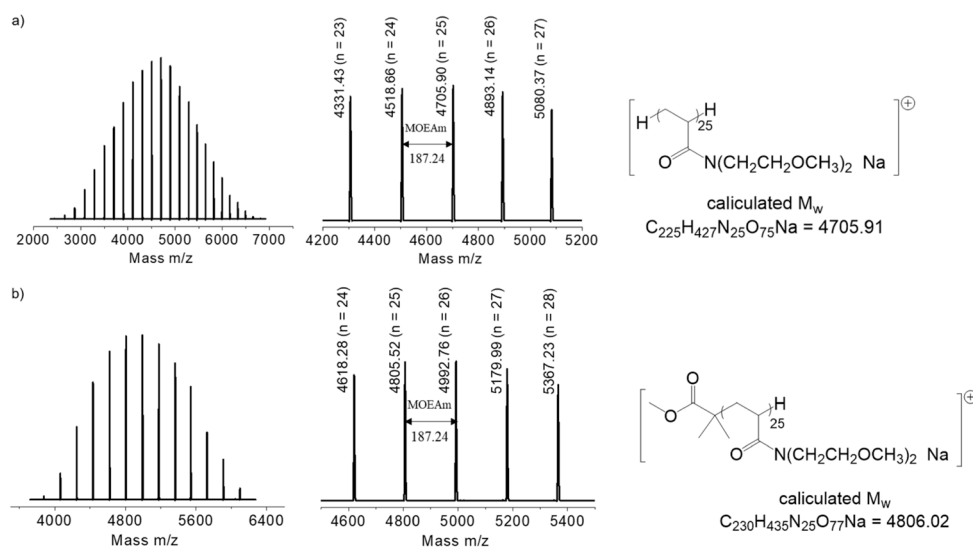


**Figure 3.** MALDI-TOF MAS spectra of (a) PMOEAm<sub>25</sub> with a  $M_{n,\text{SEC}}$  of  $4.5 \text{ kg mol}^{-1}$  and a  $\text{Đ}$  of 1.13 (Table 1, run 1) and (b) MCIP-PMOEAm<sub>25</sub> with a  $M_{n,\text{SEC}}$  of  $5.1 \text{ kg mol}^{-1}$  and a  $\text{Đ}$  of 1.11 (Table S1, run 1).

Similarly, for the polymer obtained using the conventional GTP with SKA<sup>Et</sup>, only one series of molecular ion peaks is observed in Figure 3b, and the difference in the  $m/z$  values between each peak is consistent with the molecular mass predicted for MOEAm. In addition, the  $m/z$  value of each molecular ion peak can be attributed to the sodium-cationized polymer with the MCIP group, the desilylated SKA<sup>Et</sup>, at the  $\alpha$ -chain end and a hydrogen atom at the  $\omega$ -chain end of  $[\text{CH}_3\text{O}_2\text{CC}(\text{CH}_3)_2\text{-MOEAm}_n\text{-H} + \text{Na}]^+$  ( $\text{C}_{9n+5}\text{H}_{17n+9}\text{N}_n\text{O}_{3n+2}\text{Na}$ ). For example, an  $m/z$  of 4805.52 Da for a specific peak corresponds to a  $[\text{CH}_3\text{O}_2\text{CC}(\text{CH}_3)_2\text{-MOEAm}_{25}\text{-H} + \text{Na}]^+$ .

$\text{H} + \text{Na}]^+$  with a theoretical monoisotopic value of 4806.09 for  $\text{C}_{230}\text{H}_{436}\text{N}_{25}\text{O}_{77}\text{Na}$ . In the conventional and hydrosilylation-promoted GTP reactions, the resulting polymers consisted only of monomeric units, although the difference between  $\text{Me}_2\text{EtSiH}$  and  $\text{SKA}^{\text{Et}}$  used in the initiation reaction was reflected in the structure of the initiating end of the polymer, i.e.,  $\text{PMOEAm}_{25}$  and  $\text{CH}_3\text{O}_2\text{CC}(\text{CH}_3)_2\text{-MOEAm}_{25}$ , respectively.

Furthermore, the polymerization features of the GTP of MOEAm initiated using two different methods were compared by evaluating the polymerization kinetics. The GTP of MOEAm was performed at a  $[\text{MOEAm}]_0/[\text{Me}_2\text{EtSiH} \text{ or } \text{SKA}^{\text{Et}}]_0/[\text{B}(\text{C}_6\text{F}_5)_3]_0$  ratio of 100/1/0.1 and a  $[\text{MOEAm}]_0$  of  $1.0 \text{ mol L}^{-1}$  in  $\text{CH}_2\text{Cl}_2$  at  $25^\circ\text{C}$ . Although  $\text{Et}_3\text{SiH}$  should be used for an accurate comparison with  $\text{SKA}^{\text{Et}}$ , the hydrosilylation-promoted GTP of DSAm with  $\text{Et}_3\text{SiH}$  did not proceed in a controlled/living manner; therefore,  $\text{Me}_2\text{EtSiH}$  was used instead of  $\text{Et}_3\text{SiH}$ . As shown in Figure 4, both GTP systems exhibited induction times ( $t_i$ ), with the  $t_i$  for  $\text{Me}_2\text{EtSiH}$  (13.1 min) being smaller than that for  $\text{SKA}^{\text{Et}}$  (55.0 min) due to the difference in both initiation reactions. In the kinetic plot of MOEAm with  $\text{Me}_2\text{EtSiH}$  and  $\text{SKA}^{\text{Et}}$ , a clear zero-order relationship between polymerization time and monomer conversion was observed, with  $M_{n,\text{SEC}}$  increasing linearly with increasing monomer conversion and  $\bar{D}$  remaining at low values. The polymerization rates of both GTP reactions of MOEAm were almost the same with  $k_{p,\text{obs}}$  values of  $0.35 \text{ min}^{-1}$  for  $\text{Me}_2\text{EtSiH}$  and  $0.33 \text{ min}^{-1}$  for  $\text{SKA}^{\text{Et}}$ . These results confirmed that the difference in the initiation method affected only the induction time in the early stages of the polymerization but had no effect on the propagation rate.

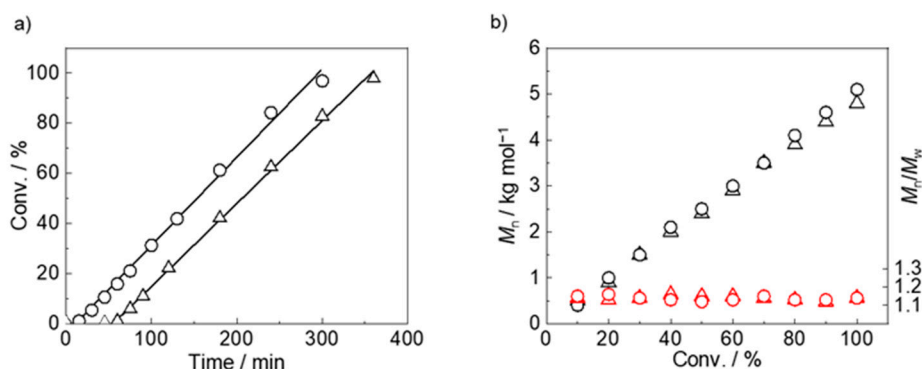


**Figure 4.** (a) Zero-order kinetic plots and (b) dependence of molar mass ( $M_n$ ) and polydispersity index ( $\bar{D}$ ) on monomer conversion (Conv.) in the  $\text{B}(\text{C}_6\text{F}_5)_3$ -catalyzed GTP of MOEAm with (○)  $\text{Me}_2\text{EtSiH}$  and (△)  $\text{SKA}^{\text{Et}}$  ( $[\text{MOEAm}]_0/[\text{Me}_2\text{EtSiH} \text{ or } \text{SKA}^{\text{Et}}]_0/[\text{B}(\text{C}_6\text{F}_5)_3]_0$ , 100/1/0.1;  $[\text{MOEAm}]_0$ ,  $1.0 \text{ mol L}^{-1}$ ).

### 3.2. Synthesis of Block and Statistical Copolymers of PMOEAm

The response performance of thermoresponsive polymers is controlled by adjusting the degree of polymerization and introducing polymer chain-end groups. The use of block and statistical copolymer systems based on thermoresponsive polymers is an additional approach to controlling the thermoresponsive property. In this study, DSAm as a simple DSAm and EOEA as an analog of MOEAm were used as comonomers. The block GTcOP reactions of MOEAm and DSAm or EOEA with  $\text{Me}_2\text{EtSiH}$  using  $\text{B}(\text{C}_6\text{F}_5)_3$  as the catalyst were performed using a sequential monomer addition method by varying the molar ratio of  $[\text{MOEAm}]_0$  and  $[\text{DSAm} \text{ or } \text{EOEA}]_0$ . The copolymerization results are listed in Tables 2 and 3, respectively.

**Table 2.** Thermoresponsive property and synthesis of PMOEAm-*b*-PDMAm and PMOEAm-*b*-PEOEAm via the hydrosilylation-promoted GTP of MOEAm with Me<sub>2</sub>EtSiH using B(C<sub>6</sub>F<sub>5</sub>)<sub>3</sub> as the catalyst, followed by the 2nd GTP of DMAm or EOEAm, respectively. <sup>a</sup>.

Run	Polymer	1st GTP <sup>b</sup>			2nd GTP <sup>c</sup>			<i>T</i> <sub>cp</sub> <sup>e</sup> /°C
		[MOEAm] <sub>0</sub> /[Me <sub>2</sub> EtSiH] <sub>0</sub>	<i>M</i> <sub>n,calcd</sub> /kg mol <sup>-1</sup>	<i>M</i> <sub>n,SEC</sub> (Đ) <sup>d</sup> /kg mol <sup>-1</sup>	[DMAm or EOEAm] <sub>0</sub>	<i>M</i> <sub>n,calcd</sub> /kg mol <sup>-1</sup>	<i>M</i> <sub>n,SEC</sub> (Đ) <sup>d</sup> /kg mol <sup>-1</sup>	
7	PMOEAm <sub>30</sub> - <i>b</i> -PDMAm <sub>70</sub>	30/1	5.6	5.5 (1.09)	70	12.5	12.5 (1.08)	- <sup>f</sup>
8	PMOEAm <sub>40</sub> - <i>b</i> -PDMAm <sub>60</sub>	40/1	7.5	7.5 (1.10)	60	13.4	13.4 (1.10)	- <sup>f</sup>
9	PMOEAm <sub>50</sub> - <i>b</i> -PDMAm <sub>50</sub>	50/1	9.4	9.6 (1.13)	50	14.3	14.4 (1.13)	58.0
10	PMOEAm <sub>60</sub> - <i>b</i> -PDMAm <sub>40</sub>	60/1	11.2	11.1 (1.10)	40	15.2	15.1 (1.09)	56.5
11	PMOEAm <sub>70</sub> - <i>b</i> -PDMAm <sub>30</sub>	70/1	13.1	12.9 (1.11)	30	16.1	16.0 (1.10)	55.8
12	PMOEAm <sub>80</sub> - <i>b</i> -PDMAm <sub>20</sub>	80/1	15.0	15.1 (1.12)	20	16.9	16.8 (1.10)	53.3
13	PMOEAm <sub>90</sub> - <i>b</i> -PDMAm <sub>10</sub>	90/1	16.8	16.7 (1.13)	10	17.8	17.6 (1.15)	51.4
14	PMOEAm <sub>30</sub> - <i>b</i> -PEOEAm <sub>70</sub>	30/1	5.6	5.3 (1.09)	70	20.7	21.0 (1.10)	- <sup>f</sup>
15	PMOEAm <sub>40</sub> - <i>b</i> -PEOEAm <sub>60</sub>	40/1	7.5	7.2 (1.08)	60	20.4	20.5 (1.09)	- <sup>f</sup>
16	PMOEAm <sub>50</sub> - <i>b</i> -PEOEAm <sub>50</sub>	50/1	9.4	9.1 (1.12)	50	20.1	20.2 (1.11)	43.5
17	PMOEAm <sub>60</sub> - <i>b</i> -PEOEAm <sub>40</sub>	60/1	11.2	10.9 (1.10)	40	19.8	19.4 (1.12)	38.0
18	PMOEAm <sub>70</sub> - <i>b</i> -PEOEAm <sub>30</sub>	70/1	13.1	12.8 (1.11)	30	19.6	19.1 (1.10)	33.5
19	PMOEAm <sub>80</sub> - <i>b</i> -PEOEAm <sub>20</sub>	80/1	15.0	15.0 (1.11)	20	19.3	19.0 (1.09)	29.7
20	PMOEAm <sub>90</sub> - <i>b</i> -PEOEAm <sub>10</sub>	90/1	16.8	16.4 (1.10)	10	19.0	18.8 (1.11)	25.0

<sup>a</sup> Solvent, CH<sub>2</sub>Cl<sub>2</sub>; [Me<sub>2</sub>EtSiH]<sub>0</sub>/[B(C<sub>6</sub>F<sub>5</sub>)<sub>3</sub>]<sub>0</sub>, 0.1; room temperature; Ar atmosphere; monomer conversion determined by <sup>1</sup>H NMR spectra in CDCl<sub>3</sub>, >99.9%. <sup>b</sup> [MOEAm]<sub>0</sub>, 1.0 mol L<sup>-1</sup>; time, 12 h and 18 h (runs 17 and 18). <sup>c</sup> [DMAm or EOEAm]<sub>0</sub> = 100 – [MOEAm]<sub>0</sub>; time, 36 h (runs 7–9), 24 h (runs 10–13), 12 h (runs 14–16), and 6 h (runs 17 and 18). <sup>d</sup> The molecular mass of the polymers was determined using size exclusion chromatography equipped with a refractive index detector in dimethylformamide (DMF) containing 0.01 mol L<sup>-1</sup> of lithium chloride and using polymethylmethacrylate (PMMA) as standards. <sup>e</sup> The cloud point temperature of [MOEAm] was determined by measuring its ultraviolet-visible spectrum in water at a concentration of 10 g L<sup>-1</sup>. <sup>f</sup> Not determined due to insoluble in water.

**Table 3.** Thermoresponsive property of PMOEAm-*s*-PDMAm and PMOEAm-*s*-PEOEAm prepared by the random hydrosilylation-promoted GTcoPs of MOEAm and DMAm or EOEAm with Me<sub>2</sub>EtSiH using B(C<sub>6</sub>F<sub>5</sub>)<sub>3</sub> as the catalyst, respectively. <sup>a</sup>.

Run	Polymer	[MOEAm + DMAm or EOEAm] <sub>0</sub> /[Me <sub>2</sub> EtSiH] <sub>0</sub>	<i>M</i> <sub>n,calcd</sub> kg mol <sup>-1</sup>	<i>M</i> <sub>n,SEC</sub> (Đ) <sup>b</sup> kg mol <sup>-1</sup>	<i>T</i> <sub>cp</sub> <sup>c</sup> °C
21	PMOEAm <sub>30</sub> - <i>s</i> -PDMAm <sub>70</sub>	(30 + 70)/1	12.5	12.5 (1.09)	- <sup>d</sup>
22	PMOEAm <sub>40</sub> - <i>s</i> -PDMAm <sub>60</sub>	(40 + 60)/1	13.4	13.6 (1.12)	73.4
23	PMOEAm <sub>50</sub> - <i>s</i> -PDMAm <sub>50</sub>	(50 + 50)/1	14.3	14.5 (1.14)	72.1
24	PMOEAm <sub>60</sub> - <i>s</i> -PDMAm <sub>40</sub>	(60 + 40)/1	15.2	15.3 (1.11)	67.5
25	PMOEAm <sub>70</sub> - <i>s</i> -PDMAm <sub>30</sub>	(70 + 30)/1	16.1	16.4 (1.15)	64.2
26	PMOEAm <sub>80</sub> - <i>s</i> -PDMAm <sub>20</sub>	(80 + 20)/1	16.9	16.6 (1.07)	59.3
27	PMOEAm <sub>90</sub> - <i>s</i> -PDMAm <sub>10</sub>	(90 + 10)/1	17.8	17.7 (1.11)	55.5
28	PMOEAm <sub>30</sub> - <i>s</i> -PEOEAm <sub>70</sub>	(30 + 70)/1	20.7	20.9 (1.15)	- <sup>e</sup>
29	PMOEAm <sub>40</sub> - <i>s</i> -PEOEAm <sub>60</sub>	(40 + 60)/1	20.4	20.6 (1.14)	- <sup>e</sup>
30	PMOEAm <sub>50</sub> - <i>s</i> -PEOEAm <sub>50</sub>	(50 + 50)/1	20.1	20.5 (1.13)	46.2
31	PMOEAm <sub>60</sub> - <i>s</i> -PEOEAm <sub>40</sub>	(60 + 40)/1	19.8	19.3 (1.09)	45.3
32	PMOEAm <sub>70</sub> - <i>s</i> -PEOEAm <sub>30</sub>	(70 + 30)/1	19.6	19.0 (1.10)	42.4
33	PMOEAm <sub>80</sub> - <i>s</i> -PEOEAm <sub>20</sub>	(80 + 20)/1	19.3	18.9 (1.12)	37.0
34	PMOEAm <sub>90</sub> - <i>s</i> -PEOEAm <sub>10</sub>	(90 + 10)/1	19.0	18.6 (1.12)	33.7

<sup>a</sup> Solvent, CH<sub>2</sub>Cl<sub>2</sub>; [MOEAm + DMAm or EOEAm]<sub>0</sub>, 1.0 mol L<sup>-1</sup>; [Me<sub>2</sub>EtSiH]<sub>0</sub>/[B(C<sub>6</sub>F<sub>5</sub>)<sub>3</sub>]<sub>0</sub>, 1; temp., 25 °C; time, 24 h; Ar atmosphere; monomer conversion determined by <sup>1</sup>H NMR spectra in CDCl<sub>3</sub>, >99.9%. <sup>b</sup> The molecular mass of the polymers was determined using size exclusion chromatography equipped with a refractive index detector in dimethylformamide (DMF) containing 0.01 mol L<sup>-1</sup> of lithium chloride and using polymethylmethacrylate (PMMA) as standards. <sup>c</sup> Determined by UV-vis measurements in water (10 g L<sup>-1</sup>). <sup>d</sup> Water-soluble but no *T*<sub>cp</sub> under 95 °C. <sup>e</sup> Not determined due to insoluble in water.

In the hydrosilylation-promoted GTcoP of MOEAm and DMAm with a [MOEAm]<sub>0</sub>/[DMAm]<sub>0</sub>/[Me<sub>2</sub>EtSiH]<sub>0</sub> molar ratio of 50/50/1 (Table 2, run 9), after confirming the quantitative consumption of MOEAm in the first GTP, DMAm was added to the living PMOEAm system to perform the second GTP. The progress of GTcoP was verified through the shift in the SEC traces of the resulting polymers between the first and second GTPs while maintaining a Đ value below 1.13, as illustrated in Figure S1. The

$M_{n,SEC}$  of the resulting polymer increased from 9.6 kg mol<sup>-1</sup> at the first GTP to 14.4 kg mol<sup>-1</sup> at the second GTP, consistent with the  $M_{n,calcd}$  values of 9.4 and 14.3 kg mol<sup>-1</sup>, respectively. Furthermore, the block GTcoP of MOEAm and EOEA<sub>m</sub> performed with a [MOEAm]<sub>0</sub>/[DMA<sub>m</sub>]<sub>0</sub>/[Me<sub>2</sub>EtSiH]<sub>0</sub> molar ratio of 50/50/1 gave similar results to the block GTcoP of MOEAm and DMA<sub>m</sub>; the  $M_{n,SEC}$  and  $\bar{D}$  values of the resulting polymers were 9.1 kg mol<sup>-1</sup> and 1.12 for the first GTP and 20.2 kg mol<sup>-1</sup> and 1.11 for the second GTP. Note that the  $M_{n,SEC}$  values were close to the  $M_{n,calcd}$  values of 9.4 and 20.1 kg mol<sup>-1</sup>, respectively. In the <sup>1</sup>H NMR spectrum of the resulting copolymer (Figure S3a), signals due to the -NCH<sub>2</sub>CH<sub>2</sub>O- and -OCH<sub>3</sub> groups were observed at 3.39–3.87 and 3.31–3.39 ppm, respectively, and a signal appearing at 2.79–3.22 ppm can be attributed to the -NCH<sub>3</sub> group of the MOEAm and DMA<sub>m</sub> units incorporated in the polymer. Similarly, signals due to the -OCH<sub>3</sub> group of PMOEAm and the -OCH<sub>2</sub>CH<sub>3</sub> group of PEOEA<sub>m</sub> were observed at 3.31–3.39 and 1.12–1.23 ppm, respectively (Figure S4a), which correspond to the MOEAm and EOEA<sub>m</sub> units incorporated in the copolymer. These results support the copolymer structures of PMOEAm<sub>50</sub>-*b*-PDMA<sub>m50</sub> and PMOEAm<sub>50</sub>-*b*-PEOEA<sub>m50</sub>. The polymerization results of the synthesis of PMOEAm<sub>x</sub>-*b*-PDMA<sub>my</sub> and PMOEAm<sub>x</sub>-*b*-PEOEA<sub>my</sub> with other x/y ratios are summarized in Table 2.

Statistical copolymers of PMOEAm-*s*-PDMA<sub>m</sub> and PMOEAm-*s*-PEOEA<sub>m</sub> were prepared via the hydrosilation-promoted GTcoP of MOEAm and DMA<sub>m</sub> or EOEA<sub>m</sub>, respectively. Table 3 lists the copolymerization results. For example, random GTcoP reactions were performed with a [MOEAm + DMA<sub>m</sub> or EOEA<sub>m</sub>]<sub>0</sub>/[Me<sub>2</sub>EtSiH]<sub>0</sub> molar ratio of (50 + 50)/1 (runs 21 and 26, respectively). The  $M_{n,SEC}$  and  $\bar{D}$  values of the resulting polymers were 14.5 kg mol<sup>-1</sup> and 1.14 (run 21) and 20.5 kg mol<sup>-1</sup> and 1.13 (run 26), with the  $M_{n,SEC}$  values agreeing with the  $M_{n,calcd}$  of 14.3 and 20.1 kg mol<sup>-1</sup>, respectively. The <sup>1</sup>H NMR spectra of both polymers with an x/y ratio of 50/50 were essentially identical to those of PMOEAm<sub>50</sub>-*b*-PDMA<sub>m50</sub> and PMOEAm<sub>50</sub>-*b*-PEOEA<sub>m50</sub> (Figures S3b and S4b, respectively). Similar to PMOEAm<sub>50</sub>-*s*-PDMA<sub>m50</sub> and PMOEAm<sub>50</sub>-*s*-PEOEA<sub>m50</sub>, other statistical copolymers with different x/y ratios were synthesized via the corresponding random GTcoP; the  $M_{n,SEC}$  values of the obtained copolymers were consistent with the  $M_{n,calcd}$  values, and the SEC traces were unimodal with low  $\bar{D}$  values (Figure S2).

The thermal phase transition behavior of a copolymer depends on the type of monomer sequence, i.e., alternating, block, or random sequence, which can be estimated by the monomer reactivity ratio ( $r$ ). Therefore, the  $r$  values of the random GTcoP of MOEAm ( $r_{MOEAm}$ ) and DMA<sub>m</sub> ( $r_{DMAm}$ ) and those of MOEAm ( $r_{MOEAm}$ ) and EOEA<sub>m</sub> ( $r_{EOEA_m}$ ) were determined using the Kelen–Tüdös method (see Supporting Information). The obtained  $r_{MOEAm}$  and  $r_{DMAm}$  values of 0.39 and 0.94, respectively, indicate that the sequence of the two monomers is relatively alternating-rich, whereas the  $r_{MOEAm}$  of 1.45 and the  $r_{EOEA_m}$  of 1.03 suggest that the sequence of the two monomers is slightly block-rich. Furthermore, the number-average sequence length of the MOEAm unit ( $l_{MOEAm}$ ) determined using the  $r$  values reflects the isolation tendency of the MOEAm–MOEAm diad. When  $x$  increased from 30 to 90 ( $x + y = 100$ ) for PMOEAm<sub>x</sub>-*s*-PDMA<sub>my</sub> and PMOEAm<sub>x</sub>-*s*-PEOEA<sub>my</sub>,  $l_{MOEAm}$  increased from 1.17 to 2.56, and  $l_{DMAm}$  decreased from 3.19 to 1.27, while  $l_{MOEAm}$  increased from 1.62 to 6.80 and  $l_{DMAm}$  decreased from 3.40 to 1.26. These results indicate that the random GTcoP of MOEAm and DMA<sub>m</sub> or EOEA<sub>m</sub> produced PMOEAm-*s*-PDMA<sub>m</sub> with an alternating-rich sequence of both monomer units and PMOEAm-*s*-PEOEA<sub>m</sub> with a block-rich sequence of both monomer units, respectively.

### 3.3. Thermoresponsive Property of PMOEAm and Its Copolymers

The thermal phase transition behavior of PMOEAm and its copolymers were assessed at  $T_{cp}$ , which is the point where the transmittance attains 50% of the transmittance-temperature curve plotted by monitoring an aqueous polymer solution (10 g L<sup>-1</sup>) using UV-vis spectroscopy at a wavelength of 500 nm. Figure S7 illustrates the findings. The thermoresponsive property of PMOEAm was compared with that of PMOEAm with the SKA residue at the  $\alpha$ -chain end and block and statistical copolymers of PMOEAm and PDMA<sub>m</sub>

or PEOEAm to investigate the effect of the chain-end group of the homopolymer and the monomer sequence of block and statistical copolymers on the thermoresponsive property. The dependence of  $T_{cp}$  on the degree of polymerization ( $DP_x$ ) for PMOEAm $_x$  and MCIP-PMOEAm $_x$  is shown in Figure 5a. The  $T_{cp}$  of both polymers decreased as  $DP_x$  increased, from 56.5 °C to 48.0 °C for PMOEAm $_x$  and from 41.5 °C to 34.5 °C for MCIP-PMOEAm $_x$ . The relationship between  $DP_x$  and  $T_{cp}$  for both polymers was very similar, but the  $T_{cp}$  of MCIP-PMOEAm $_x$  was, on average, 13.4 °C lower than that of PMOEAm $_x$ , regardless of the  $DP_x$ . These results indicate that the  $-C(CH_3)_2$  group acted as a hydrophobic group, reducing the  $T_{cp}$  of PMOEAm $_x$ . Therefore, a polymer without substituents at the chain ends should be used to determine whether the polymer exhibits thermoresponsive properties. The thermal phase transition should be accompanied by a change in the aggregate size of the copolymers, which was confirmed by measuring their hydrodynamic radius ( $R_h$ ) in water before and after the  $T_{cp}$ . The  $R_h$  values increased drastically from 15.2 nm at 20 °C to 425.6 nm at 60 °C for the PMOEAm $_{50}$  polymer with a  $T_{cp}$  of 53.9 °C and from 16.1 nm at 20 °C to 457.2 nm at 60 °C for the MCIP-PMOEAm $_{50}$  polymer with a  $T_{cp}$  of 40.8 °C (Table 4).

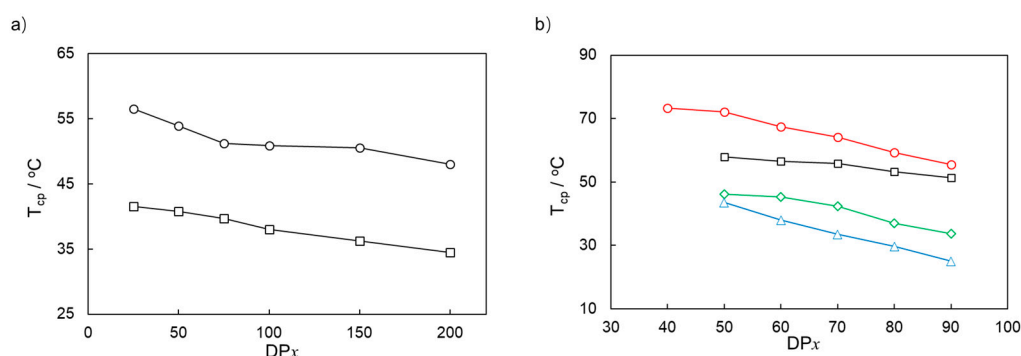


**Figure 5.** Dependence of  $T_{cp}$  on  $DP_x$  for (a) (○) PMOEAm $_x$  and (□) MCIP-PMOEAm $_x$  and (b) (○) PMOEAm $_x$ -s-PDMAm $_y$ , (□) PMOEAm $_x$ -b-PDMAm $_y$ , (◇) PMOEAm $_x$ -s-PEOEAm $_y$ , and (△) PMOEAm $_x$ -b-PEOEAm $_y$ .

**Table 4.**  $R_h$  values for PMOEAm $_{50}$ , MCIP-PMOEAm $_{50}$ , PMOEAm $_{50}$ -b-PDMAm $_{50}$ , PMOEAm $_{50}$ -s-PDMAm $_{50}$ , PMOEAm $_{50}$ -b-PEOEAm $_{50}$ , and PMOEAm $_{50}$ -s-PEOEAm $_{50}$  at 20 °C and 60 °C.

Polymer Code	$T_{cp}$ <sup>a</sup>	$R_h$ <sup>b</sup> /nm	
		20 °C	60 °C
PMOEAm $_{50}$	53.9	15.2	425.6
MCIP-PMOEAm $_{50}$	40.8	16.1	457.2
PMOEAm $_{50}$ -b-PDMAm $_{50}$	58.0	16.7	402.8
PMOEAm $_{50}$ -s-PDMAm $_{50}$	72.1	14.5	349.3 <sup>c</sup>
PMOEAm $_{50}$ -b-PEOEAm $_{50}$	25.0	18.9	551.7
PMOEAm $_{50}$ -s-PEOEAm $_{50}$	33.7	18.3	482.6

<sup>a</sup> The cloud point temperature of [MOEAm] was determined by measuring its ultraviolet-visible spectrum in water at a concentration of 10 g L<sup>-1</sup>. <sup>b</sup> Determined by DLS measurements in 10 g L<sup>-1</sup> water by dynamic light scattering (DLS). <sup>c</sup> At 75 °C.

For all copolymer systems, the  $T_{cp}$  increased with a decreasing  $DP_x$  from 51.4 °C to 58.0 °C for PMOEAm $_x$ -b-PDMAm $_y$ , from 55.5 °C to 73.4 °C for PMOEAm $_x$ -s-PDMAm $_y$ , from 25.0 °C to 43.5 °C for PMOEAm $_x$ -b-PEOEAm $_y$ , and from 33.7 °C to 46.2 °C for PMOEAm $_x$ -s-PEOEAm $_y$  (Figures 5 and 6b). PDMAm is nonthermoresponsive and highly water soluble, whereas PEOEAm is thermoresponsive with a low  $T_{cp}$  and less water soluble. This is reflected in the  $T_{cp}$  of the block and statistical copolymers of PMOEAm-b-PDMAm and PMOEAm $_x$ -s-PDMAm, which were higher than those of PMOEAm-b-PEOEAm and PMOEAm-s-PEOEAm. For PMOEAm and its block and statistical copolymers, the  $T_{cp}$

increased slightly from 53.9 °C for PMOEA<sub>m50</sub> to 58.0 °C for PMOEA<sub>m50</sub>-*b*-PDMAm<sub>50</sub> and increased considerably to 72.1 °C for PMOEA<sub>m50</sub>-*s*-PDMAm<sub>50</sub> due to the alternating-rich monomer sequence. Meanwhile, the  $T_{cp}$  decreased from 53.9 °C for PMOEA<sub>m50</sub> to 43.5 °C for PMOEA<sub>m50</sub>-*b*-PDMAm<sub>50</sub> and increased slightly to 46.2 °C for PMOEA<sub>m50</sub>-*s*-PEOEA<sub>m50</sub>. The slight difference in  $T_{cp}$  between the block and statistical copolymers can be attributed to the lower degree of blockiness in the monomer sequence in the statistical copolymer.

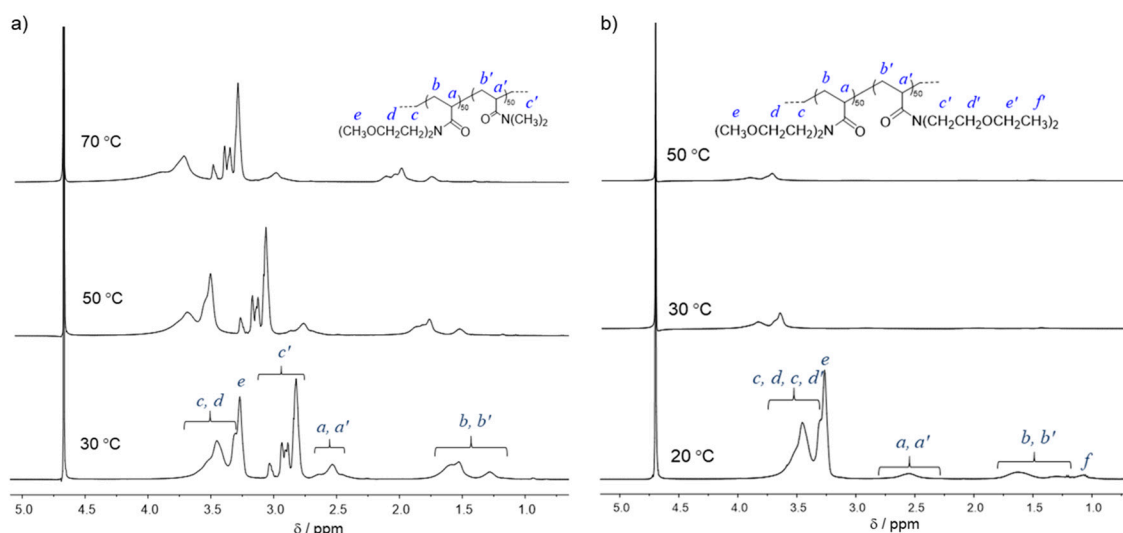


**Figure 6.** <sup>1</sup>H NMR spectra of (a) PMOEA<sub>50</sub>-*b*-PDMAm<sub>50</sub> measured in D<sub>2</sub>O at 30, 50, and 70 °C and (b) PMOEA<sub>50</sub>-*b*-PEOEA<sub>50</sub> measured in D<sub>2</sub>O at 20, 30, and 50 °C.

The phase transition behavior was confirmed by measuring <sup>1</sup>H NMR spectra at different temperatures. In the <sup>1</sup>H NMR spectra of PMOEA<sub>50</sub>-*b*-PDMAm<sub>50</sub> with a  $T_{cp}$  of 58.0 °C, signals attributed to the -OCH<sub>3</sub> group of PMOEA<sub>m</sub> and the -NCH<sub>3</sub> group of PDMAm were observed at 3.19–3.30 and 2.73–3.07 ppm, respectively, at 30 °C. These signals shifted to a low magnetic field, and the intensity of the signal of the -OCH<sub>3</sub> group decreased compared with that of the -NCH<sub>3</sub> group at 50 °C. The signal of the -OCH<sub>3</sub> group completely disappeared at 75 °C. A similar thermal phase transition was observed for PMOEA<sub>50</sub>-*s*-PDMAm<sub>50</sub> with a  $T_{cp}$  of 72.1 °C (Figure S5). Furthermore, an increase in  $R_h$  from 16.7 nm at 20 °C to 402.8 nm at 70 °C for PMOEA<sub>50</sub>-*b*-PDMAm<sub>50</sub> and from 14.5 nm at 20 °C to 349.9 nm at 75 °C for PMOEA<sub>50</sub>-*s*-PDMAm<sub>50</sub> was observed. These results indicate that PMOEA<sub>m</sub> and PDMAm acted as hydrophobic and hydrophilic moieties, respectively, resulting in the formation of aggregates comprising a PMOEA<sub>m</sub> core and a PDMAm shell. In the <sup>1</sup>H NMR spectra in the D<sub>2</sub>O of PMOEA<sub>50</sub>-*b*-PEOEA<sub>50</sub> with a  $T_{cp}$  of 25.0 °C (Figure 5b), the signal at 1.11 ppm attributed to the -OCH<sub>2</sub>CH<sub>3</sub> groups of PEOEA<sub>m</sub> decreased at 20 °C and disappeared completely at 30 °C, which may be partly due to the low  $T_{cp}$  of 13.9 °C for the PEOEA<sub>m50</sub> moiety. A signal due to the -OCH<sub>3</sub> of PMOEA<sub>m</sub> observed at 3.27 ppm at 20 °C decreased considerably at 30 °C and disappeared completely at 50 °C. A similar thermal phase transition was observed in the <sup>1</sup>H NMR spectra of PMOEA<sub>50</sub>-*s*-PEOEA<sub>50</sub> with a  $T_{cp}$  of 46.2 °C (Figure S5). However, an increase in  $R_h$  from 16.7 nm at 20 °C to 402.8 nm at 60 °C for PMOEA<sub>50</sub>-*b*-PEOEA<sub>50</sub> and from 18.9 nm at 20 °C to 551.7 nm at 60 °C for PMOEA<sub>50</sub>-*s*-PEOEA<sub>50</sub> confirmed the thermal phase transition. In the block and statistical copolymers of PEOEA<sub>m</sub> and PMOEA<sub>m</sub>, the small change in  $T_{cp}$  is due to PEOEA<sub>m</sub> with a low  $T_{cp}$  acting as a highly hydrophobic moiety.

#### 4. Conclusions

Using the conventional method with SKA<sup>Et</sup> and the hydrosilylation-promoted method with Me<sub>2</sub>EtSiH, we proceeded in a controlled/living manner to produce PMOEA<sub>m</sub> and

MCIP-PMOEAm, respectively. Using a different initiation method affected only the induction time in the early stages of the polymerization, whereas it had no effect on the propagation rate. The relationship between  $DP_x$  and  $T_{cp}$  for PMOEAm<sub>x</sub> and MCIP-PMOEAm<sub>x</sub> was very similar, but the  $T_{cp}$  of MCIP-PMOEAm<sub>x</sub> was lower than that of PMOEAm<sub>x</sub>, regardless of the  $DP_x$  value. Poly(*N,N*-disubstituted acrylamide), a polymer segment combined in copolymers of PMOEAm, affected the thermoresponsive properties, with the  $T_{cp}$  of the block and statistical copolymers consisting of PMOEAm, and nonthermoresponsive and highly water-soluble PDMAm being higher than that of copolymers with thermoresponsive and less water-soluble PEOEAm. For PMOEAm and its block and statistical copolymers, the  $T_{cp}$  was slightly higher for PMOEAm-*b*-PDMAm than for PMOEAm and considerably higher for PMOEAm-*s*-PDMAm due to the alternating-rich nature of the monomer sequence. Meanwhile, the difference in  $T_{cp}$  was small between PMOEAm, PMOEAm-*b*-PEOEAm, and PMOEAm-*s*-PEOEAm, and the DP dependence on  $T_{cp}$  was small for these (co)polymers. These thermoresponsive features are most likely caused by the low  $T_{cp}$  of PEOEAm. To determine whether a polymer exhibits thermoresponsive properties and the type of comonomers that are appropriate to obtain thermoresponsive copolymers, polymers without substituents at the chain ends should be used. Hydrosilylation-promoted GTP is a reliable tool for resolving these issues and will contribute to the molecular design, synthesis, and application of thermoresponsive polymer materials.

**Supplementary Materials:** The following supporting information can be downloaded at <https://www.mdpi.com/article/10.3390/polym15244681/s1>: Table S1. Synthesis of MCIP-PMOEAm by GTP of MOEAm with SKA<sup>Et</sup> using B(C<sub>6</sub>F<sub>5</sub>)<sub>3</sub> as the catalyst.; Table S2. Random group transfer copolymerization (GTcoP) of MOEAm and DMAM with Me<sub>2</sub>EtSiH using B(C<sub>6</sub>F<sub>5</sub>)<sub>3</sub> as the catalyst.; Table S3. Random group transfer copolymerization (GTcoP) of MOEAm and EOEAm with Me<sub>2</sub>EtSiH using B(C<sub>6</sub>F<sub>5</sub>)<sub>3</sub> as the catalyst.; Figure S1. SEC traces of PMOEAm<sub>x</sub>-*b*-PDMAm<sub>y</sub> with (a)  $x/y = 30/70$ , (b)  $x/y = 40/60$ , (c)  $x/y = 50/50$ , (d)  $x/y = 60/40$ , (e)  $x/y = 70/30$ , (f)  $x/y = 80/20$ , and (g)  $x/y = 90/10$  and PMOEAm<sub>x</sub>-*b*-PEOEAm<sub>y</sub> with (h)  $x/y = 50/50$ , (i)  $x/y = 60/40$ , (j)  $x/y = 70/30$ , (k)  $x/y = 80/20$ , and (l)  $x/y = 90/10$  (eluent, DMF containing lithium chloride (0.01 mol L<sup>-1</sup>); flow rate, 1.0 mL min<sup>-1</sup>); Figure S2. SEC traces of PMOEAm<sub>x</sub>-*s*-PDMAm<sub>y</sub> with (a)  $x/y = 30/70$ , (b)  $x/y = 40/60$ , (c)  $x/y = 50/50$ , (d)  $x/y = 60/40$ , (e)  $x/y = 70/30$ , (f)  $x/y = 80/20$ , and (g)  $x/y = 90/10$  and PMOEAm<sub>x</sub>-*s*-PEOEAm<sub>y</sub> with (h)  $x/y = 50/50$ , (i)  $x/y = 60/40$ , (j)  $x/y = 70/30$ , (k)  $x/y = 80/20$ , and (l)  $x/y = 90/10$  (eluent, DMF containing lithium chloride (0.01 mol L<sup>-1</sup>); flow rate, 1.0 mL min<sup>-1</sup>); Figure S3. <sup>1</sup>H NMR spectra of (a) PMOEAm<sub>50</sub>-*b*-PDMAm<sub>50</sub> and (b) PMOEAm<sub>50</sub>-*s*-PDMAm<sub>50</sub> in CDCl<sub>3</sub>; Figure S4. <sup>1</sup>H NMR spectra of (a) PMOEAm<sub>50</sub>-*b*-PEOEAm<sub>50</sub> and (b) PMOEAm<sub>50</sub>-*s*-PEOEAm<sub>50</sub> in CDCl<sub>3</sub>; Figure S5. <sup>1</sup>H NMR spectra of PMOEAm<sub>50</sub>-*s*-PDMAm<sub>50</sub> measured at 20, 30, and 50 °C in D<sub>2</sub>O; Figure S6. <sup>1</sup>H NMR spectra of PMOEAm<sub>50</sub>-*s*-PEOEAm<sub>50</sub> measured at 20, 35, and 50 °C in D<sub>2</sub>O; Figure S7. UV-vis absorption spectra of (a) PMOEAm, (b) MCIP-PMOEAm, (c) PMOEAm-*s*-PDMAm, (d) PMOEAm-*b*-PDMAm, (e) PMOEAm-*s*-PEOEAm, and (f) PMOEAm-*b*-PEOEAm in water (10 g L<sup>-1</sup>) at different temperatures.; Figure S8.  $R_h$  values for (a) PMOEAm<sub>50</sub>, (b) MCIP-PMOEAm<sub>50</sub>, (c) PMOEAm<sub>50</sub>-*s*-PDMAm<sub>50</sub>, (d) PMOEAm<sub>50</sub>-*b*-PDMAm<sub>50</sub>, (e) PMOEAm<sub>50</sub>-*s*-PEOEAm<sub>50</sub>, and (f) PMOEAm<sub>50</sub>-*b*-PEOEAm<sub>50</sub> at 20 and 60 °C.

**Author Contributions:** Data curation, writing—original draft preparation, X.F.; validation, Y.W.; data curation, L.X.; methodology, A.N.; validation and funding acquisition, S.-i.S.; data curation and funding acquisition, X.Y.; project administration and funding acquisition, X.S.; writing—review, data curation and editing, T.K. All authors have read and agreed to the published version of the manuscript.

**Funding:** This research was funded by the Recruitment Program of Global Experts, China; Science and Technology Department of Jilin Province, grant number KYC-JC-XM-2023-093; Jilin Provincial Department Of Education Fund, grant number 6012100010111, and the Youth Fund of Changchun University Of Science And Technology, grant number 201905010029; National Natural Science Foundation of China, grant number 52173202; the Heilongjiang Science Foundation Project, grant number YQ2022E043; Science and Technology Department of Jilin Province, grant number YDZJ202301ZYTS298; the Fundamental Research Funds in Heilongjiang Provincial Universities, grant number 145209131; Grant-in-Aid for Challenging Exploratory Research (22K19929029) from JSPS, Japan.

**Institutional Review Board Statement:** Not applicable.

**Data Availability Statement:** Data are contained within the article and supplementary materials.

**Conflicts of Interest:** The authors declare no conflict of interest.

## References

1. Watanabe, E.; Tomoshige, N.; Uyama, H. New Biodegradable and Thermo-responsive Polymers Based on Amphiphilic Poly(asparagine) Derivatives. *Macromol. Symp.* **2007**, *249–250*, 509–514. [[CrossRef](#)]
2. Pasparakis, G.; Tsitsilianis, C. LCST Polymers: Thermo-responsive Nanostructured Assemblies towards Bioapplications. *Polymer* **2020**, *211*, 123146. [[CrossRef](#)]
3. Lang, X.; Patrick, A.D.; Hammouda, B.; Hore, M.J.A. Chain terminal group leads to distinct thermo-responsive behaviors of linear PNIPAM and polymer analogs. *Polymer* **2018**, *145*, 137–147. [[CrossRef](#)]
4. Schroffenegger, M.; Reimhult, E. Thermo-responsive Core-Shell Nanoparticles: Does Core Size Matter? *Materials* **2018**, *11*, 1654. [[CrossRef](#)] [[PubMed](#)]
5. Nobuyuki, H.; Sho, M.; Shin-nosuke, N.; Tomoyuki, K. Stepwise Thermo-Responsive Amino Acid-Derived Triblock Vinyl Polymers: ATRP Synthesis of Polymers, Aggregation, and Gelation Properties via Flower-Like Micelle Formation. *Materials* **2018**, *11*, 424.
6. Boutris, C.; Chatzi, E.G.; Kiparissides, C. Characterization of the LCST behaviour of aqueous poly(N-isopropylacrylamide) solutions by thermal and cloud point techniques. *Polymer* **1997**, *38*, 2567–2570. [[CrossRef](#)]
7. Ni, C.H.; Zhu, X.X.; Wang, Q.L.; Zeng, X.Y. Studies on LCST of poly(N-isopropylacrylamide-co-acrylic acid-co-N-diacetone acrylamide). *Chin. Chem. Lett.* **2007**, *18*, 79–80. [[CrossRef](#)]
8. Liu, X.; Song, T.; Chang, M.; Meng, L.; Wang, X.; Sun, R.; Ren, J. Carbon Nanotubes Reinforced Maleic Anhydride-Modified Xylan-g-Poly(N-isopropylacrylamide) Hydrogel with Multifunctional Properties. *Materials* **2018**, *11*, 354. [[CrossRef](#)]
9. Saremi, B.; Yao, T.; Yuan, B. Thermo- and pH-sensitive nanoparticles of poly (N-isopropylacrylamide-decenoic acid-1-vinylimidazole) for ultrasound switchable fluorescence imaging. *Exp. Biol. Med.* **2022**, *247*, 1005–1012. [[CrossRef](#)]
10. Li, S.; Song, F.; Sun, C.; Hu, J.; Zhang, Y. Amphiphilic methoxy poly(ethylene glycol)-b-poly(carbonate-selenide) with enhanced ROS responsiveness: Facile synthesis and oxidation process. *Eur. Polym. J.* **2021**, *159*, 110752. [[CrossRef](#)]
11. Son, K.; Lee, J. Synthesis and Characterization of Poly(Ethylene Glycol) Based Thermo-Responsive Hydrogels for Cell Sheet Engineering. *Materials* **2016**, *9*, 854. [[CrossRef](#)]
12. Gordon, T.N.; Kornmuller, A.; Soni, Y.; Flynn, L.E.; Gillies, E.R. Polyesters based on aspartic acid and poly(ethylene glycol): Functional polymers for hydrogel preparation. *Eur. Polym. J.* **2021**, *152*, 110456. [[CrossRef](#)]
13. Kabra, B.G.; Gehrke, S.H.; Hwang, S.T.; Ritschel, W.A. Modification of the dynamic swelling behavior of poly(2-hydroxyethyl methacrylate) in water. *J. Appl. Polym. Sci.* **1991**, *42*, 2409–2416. [[CrossRef](#)]
14. Moynihan, H.J.; Honey, M.S.; Peppas, N.A. Solute diffusion in swollen membranes. Part V: Solute diffusion in poly(2-hydroxyethyl methacrylate). *Polym. Eng. Sci.* **1986**, *26*, 1180–1185. [[CrossRef](#)]
15. Choudhury, N.; Das, S.; Samadder, S.; De, P. Phenylalanine-Tethered pH-Responsive Poly(2-Hydroxyethyl Methacrylate). *Chem. Asian J.* **2021**, *16*, 1016–1024. [[CrossRef](#)]
16. Liu, S.; Liu, M. Synthesis and characterization of temperature- and pH-sensitive poly(N,N-diethylacrylamide-co-methacrylic acid). *J. Appl. Polym. Sci.* **2003**, *90*, 3563–3568. [[CrossRef](#)]
17. Constantin, M.; Bucatariu, S.; Harabagiu, V.; Popescu, I.; Ascenzi, P.; Fundueanu, G. Poly(N-isopropylacrylamide-co-methacrylic acid) pH/thermo-responsive porous hydrogels as self-regulated drug delivery system. *Eur. J. Pharm. Sci.* **2014**, *62*, 86–95. [[CrossRef](#)] [[PubMed](#)]
18. Noël, M.-H.; van Damme, H.; Hébraud, P. Building of a thermo-responsive cement. *Cem. Concr. Res.* **2011**, *41*, 975–980. [[CrossRef](#)]
19. Shi, J.; Wang, X.; Xu, S.; Wu, Q.; Cao, S. Reversible thermal-tunable drug delivery across nano-membranes of hollow PUA/PSS multilayer microcapsules. *J. Membr. Sci.* **2016**, *499*, 307–316. [[CrossRef](#)]
20. Bercea, M.; Nita, L.-E.; Eckelt, J.; Wolf, B.A. Polyelectrolyte Complexes: Phase Diagram and Intrinsic Viscosities of the System Water/Poly(2-vinylpyridinium-Br)/Poly(styrene sulfonate-Na). *Macromol. Chem. Phys.* **2012**, *213*, 2504–2513. [[CrossRef](#)]
21. An, Q.; Beh, C.; Xiao, H. Preparation and characterization of thermo-sensitive poly(vinyl alcohol)-based hydrogel as drug carrier. *J. Appl. Polym. Sci.* **2013**, *131*, 39720. [[CrossRef](#)]
22. Petrov, S.; Ivanova, T.; Christova, D.; Ivanova, S. Modification of polyacrylonitrile membranes with temperature sensitive poly(vinylalcohol-co-vinylacetal). *J. Membr. Sci.* **2005**, *261*, 1–6. [[CrossRef](#)]
23. Liu, J.; Detrembleur, C.; Hurtgen, M.; Debuigne, A.; De Pauw-Gillet, M.-C.; Mornet, S.; Jérôme, C. Thermo-responsive gold/poly(vinyl alcohol)-b-poly(N-vinylcaprolactam) core-crown nanoparticles as a drug delivery system. *Polym. Chem.* **2014**, *5*, 5289–5299. [[CrossRef](#)]
24. Cheng, S.; Feng, W.; Pashikin, I.; Yuan, L.; Deng, H.; Zhou, Y. Radiation polymerization of thermo-sensitive poly(N-vinylcaprolactam). *Radiat. Phys. Chem.* **2002**, *63*, 517–519. [[CrossRef](#)]
25. Medeiros, S.F.; Barboza, J.C.S.; Giudici, R.; Santos, A.M. Thermally-sensitive and Biocompatible Poly(N-vinylcaprolactam): A Kinetic Study of Free Radical Polymerization in Ethanol. *J. Macromol. Sci. A* **2013**, *50*, 763–773. [[CrossRef](#)]

26. Winninger, J.; Iurea, D.M.; Atanase, L.I.; Salhi, S.; Delaite, C.; Riess, G. Micellization of novel biocompatible thermo-sensitive graft copolymers based on poly( $\epsilon$ -caprolactone), poly(N-vinylcaprolactam) and poly(N-vinylpyrrolidone). *Eur. Polym. J.* **2019**, *119*, 74–82. [[CrossRef](#)]
27. Zhang, X.; Burton, T.F.; In, M.; Bégu, S.; Aubert-Pouëssel, A.; Robin, J.-J.; Giani, O. Synthesis and behavior of PEG-b-PDEAm block copolymers in aqueous solution. *Mater. Today Commun.* **2020**, *24*, 100987. [[CrossRef](#)]
28. Chen, J.; Liu, M.; Jin, S.; Liu, H. Synthesis and characterization of  $\kappa$ -carrageenan/poly(N,N-diethylacrylamide) semi-interpenetrating polymer network hydrogels with rapid response to temperature. *Polym. Adv. Technol.* **2008**, *19*, 1656–1663. [[CrossRef](#)]
29. Ward, M.A.; Georgiou, T.K. Thermoresponsive Polymers for Biomedical Applications. *Polymers* **2011**, *3*, 1215–1242. [[CrossRef](#)]
30. Zhu, J.; Zhang, G.; Li, J. Preparation of amphoteric polyacrylamide flocculant and its application in the treatment of tannery wastewater. *J. Appl. Polym. Sci.* **2010**, *120*, 518–523. [[CrossRef](#)]
31. Danch, A.; Laggner, P.; Degovics, G.; Sek, D.; Stelzer, F. Thermodynamic and structure investigations of new side-chain liquid crystal polymer. *Proc. SPIE-Int. Soc. Opt. Eng.* **1998**, *3319*, 271–275.
32. Biswas, C.S.; Hazer, B. Synthesis and characterization of stereoregular poly(N-ethylacrylamide) hydrogel by using Y(OTf)<sub>3</sub> Lewis acid. *Colloid Polym. Sci.* **2014**, *293*, 143–152. [[CrossRef](#)]
33. Liu, C.; Wang, S.; Zhou, H.; Gao, C.; Zhang, W. Thermoresponsive poly(ionic liquid): Controllable RAFT synthesis, thermoresponse, and application in dispersion RAFT polymerization. *J. Polym. Sci. Part A Polym. Chem.* **2015**, *54*, 945–954. [[CrossRef](#)]
34. Li, Y.; Wang, F.; Sun, T.; Du, J.; Yang, X.; Wang, J. Surface-modulated and thermoresponsive polyphosphoester nanoparticles for enhanced intracellular drug delivery. *Sci. China Chem.* **2014**, *57*, 579–585. [[CrossRef](#)]
35. Cheng, C.; Wei, H.; Shi, B.-X.; Cheng, H.; Li, C.; Gu, Z.-W.; Zhuo, R.-X.; Zhang, X.-Z.; Zhuo, R.-X. Biotinylated thermoresponsive micelle self-assembled from double-hydrophilic block copolymer for drug delivery and tumor target. *Biomaterials* **2008**, *29*, 497–505. [[CrossRef](#)]
36. Kwon, I.K.; Matsuda, T. Photo-iniferter-based thermoresponsive block copolymers composed of poly(ethylene glycol) and poly(N-isopropylacrylamide) and chondrocyte immobilization. *Biomaterials* **2006**, *27*, 986–995. [[CrossRef](#)]
37. Porjazoska, A.; Dimitrov, P.; Dimitrov, I.; Cvetkovska, M.; Tsvetanov, C.B. Synthesis and aqueous solution properties of functionalized and thermoresponsive poly(D,L-lactide)/polyether block copolymers. *Macromol. Symp.* **2004**, *210*, 427–436. [[CrossRef](#)]
38. Peleshanko, S.; Anderson, K.D.; Goodman, M.; Determan, M.D.; Mallapragada, S.K.; Tsukruk, V.V. Thermoresponsive Reversible Behavior of Multistimuli Pluronic-Based Pentablock Copolymer at the Air–Water Interface. *Langmuir* **2007**, *23*, 25–30. [[CrossRef](#)]
39. Yoshioka, H.; Mikami, M.; Mori, Y.; Tsuchida, E. Preparation of thermoresponsive surfaces using polyvinylchloride-graft-poly(N-isopropylacrylamide). *Polym. Adv. Technol.* **1993**, *4*, 519–521. [[CrossRef](#)]
40. Oh, B.H.L.; Bismarck, A.; Chan-Park, M.B. High Internal Phase Emulsion Templating with Self-Emulsifying and Thermoresponsive Chitosan-graft-PNIPAM-graft-Oligoproline. *Biomacromolecules* **2014**, *15*, 1777–1787. [[CrossRef](#)]
41. Wu, Y.; Deng, Y.; Yuan, Q.; Ling, Y.; Tang, H. Thermoresponsive poly( $\gamma$ -propyl-L-glutamate)-graft-(oligo ethylene glycol): Synthesis, characterization, and properties. *J. Appl. Polym.* **2014**, *131*, 41022. [[CrossRef](#)]
42. Kelland, M.A. Tuning the thermoresponsive properties of hyperbranched poly(ester amide)s based on diisopropanolamine and cyclic dicarboxylic anhydrides. *J. Appl. Polym.* **2011**, *121*, 2282–2290. [[CrossRef](#)]
43. Tong, J.; Wei, Z.; Yang, L.; Yang, Y.; Chen, Y. Study on the phase transition behaviors of thermoresponsive hyperbranched polyampholytes in water. *Polymer* **2016**, *84*, 107–116. [[CrossRef](#)]
44. Rezaei, S.J.T.; Nabid, M.R.; Niknejad, H.; Entezami, A.A. Folate-decorated thermoresponsive micelles based on star-shaped amphiphilic block copolymers for efficient intracellular release of anticancer drugs. *Int. J. Pharm.* **2012**, *437*, 70–79. [[CrossRef](#)]
45. Ida, S.; Toyama, Y.; Takeshima, S.; Kanaoka, S. Thermoresponsive core cross-linked star-shaped poly(N-isopropylacrylamide) for reversible and controlled aggregation of nanoscale molecular units. *Polym. J.* **2019**, *52*, 359–363. [[CrossRef](#)]
46. Ma, C.; Han, T.; Niu, N.; Al-Shok, L.; Efstathiou, S.; Lester, D.W.; Huband, S.; Haddleton, D. Well-defined polyacrylamides with AIE properties via rapid Cu-mediated living radical polymerization in aqueous solution: Thermoresponsive nanoparticles for bioimaging. *Polym. Chem.* **2021**, *13*, 58–68. [[CrossRef](#)]
47. Zhang, C.; Maric, M. Fluorescent, thermoresponsive copolymers via nitroxide-mediated polymerization: Synthesis and effect of fluorescent groups on phase transitions in an ionic liquid. *J. Polym. Sci. A Polym. Chem.* **2013**, *51*, 4702–4715. [[CrossRef](#)]
48. Kwan, S.; Marić, M. Thermoresponsive polymers with tunable cloud point temperatures grafted from chitosan via nitroxide mediated polymerization. *Polymer* **2016**, *86*, 69–82. [[CrossRef](#)]
49. Kim, D.J.; Kang, S.M.; Kong, B.; Kim, W.-J.; Paik, H.; Choi, H.; Choi, I.S. Formation of Thermoresponsive Gold Nanoparticle/PNIPAAm Hybrids by Surface-Initiated, Atom Transfer Radical Polymerization in Aqueous Media. *Macromol. Chem. Phys.* **2005**, *206*, 1941–1946. [[CrossRef](#)]
50. Zhang, K.; Ma, J.; Zhang, B.; Zhao, S.; Li, Y.; Xu, Y.; Wang, J. Synthesis of thermoresponsive silica nanoparticle/PNIPAM hybrids by aqueous surface-initiated atom transfer radical polymerization. *Mater. Lett.* **2007**, *61*, 949–952. [[CrossRef](#)]
51. Kim, Y.S.; Kadla, J.F. Preparation of a Thermoresponsive Lignin-Based Biomaterial through Atom Transfer Radical Polymerization. *Biomacromolecules* **2010**, *11*, 981–988. [[CrossRef](#)]
52. Kessel, S.; Truong, N.P.; Jia, Z.; Monteiro, M.J. Aqueous reversible addition-fragmentation chain transfer dispersion polymerization of thermoresponsive diblock copolymer assemblies: Temperature directed morphology transformations. *J. Polym. Sci. A Polym. Chem.* **2012**, *50*, 4879–4887. [[CrossRef](#)]

53. Pascual, S.; Monteiro, M.J. Shell-crosslinked nanoparticles through self-assembly of thermoresponsive block copolymers by RAFT polymerization. *Eur. Polym. J.* **2009**, *45*, 2513–2519. [[CrossRef](#)]
54. Liu, H.; Zhang, J.; Luo, X.; Kong, N.; Cui, L.; Liu, J. Preparation of biodegradable and thermoresponsive enzyme–polymer conjugates with controllable bioactivity via RAFT polymerization. *Eur. Polym. J.* **2013**, *49*, 2949–2960. [[CrossRef](#)]
55. Webster, O.W. Molecular architecture control in acrylic polymers by group transfer polymerization. *Macromol. Symp.* **1993**, *70–71*, 75–81. [[CrossRef](#)]
56. Raynaud, J.; Ciolino, A.; Baceiredo, A.; Destarac, M.; Bonnette, F.; Kato, T.; Taton, D. Harnessing the Potential of N-Heterocyclic Carbenes for the Rejuvenation of Group-Transfer Polymerization of (Meth)Acrylics. *Angew. Chem. Int. Ed.* **2008**, *47*, 5390–5393. [[CrossRef](#)]
57. Scholten, M.D.; Hedrick, J.L.; Waymouth, R.M. Group Transfer Polymerization of Acrylates Catalyzed by N-Heterocyclic Carbenes. *Macromolecules* **2008**, *41*, 7399–7404. [[CrossRef](#)]
58. Liu, Y.; Li, Y.; Chen, Y. Organocatalyzed Group Transfer Polymerization of Alkyl Sorbate: Polymer Synthesis, Postpolymerization Modification, and Thermal Properties. *Macromolecules* **2021**, *54*, 9039–9052. [[CrossRef](#)]
59. Ute, K.; Tarao, T.; Nakao, S.; Kitayama, T. Preparation and properties of disyndiotactic poly(alkylcrotonate)s. *Polymer* **2003**, *44*, 7869–7874. [[CrossRef](#)]
60. Raynaud, J.; Liu, N.; Fèvre, M.; Gnanou, Y.; Taton, D. No matter the order of monomer addition for the synthesis of well-defined block copolymers by sequential group transfer polymerization using N-heterocyclic carbenes as catalysts. *Polym. Chem.* **2011**, *2*, 1706. [[CrossRef](#)]
61. Kikuchi, S.; Chen, Y.; Ichinohe, E.; Kitano, K.; Sato, S.; Duan, Q.; Shen, X.; Kakuchi, T. Synthesis and Thermoresponsive Property of Linear, Cyclic, and Star-Shaped Poly(N,N-diethylacrylamide)s Using B(C<sub>6</sub>F<sub>5</sub>)<sub>3</sub>-Catalyzed Group Transfer Polymerization as Facile End-Functionalization Method. *Macromolecules* **2016**, *49*, 4828–4838. [[CrossRef](#)]
62. Chen, Y.; Kitano, K.; Tsuchida, S.; Kikuchi, S.; Takada, K.; Satoh, T.; Kakuchi, T. B(C<sub>6</sub>F<sub>5</sub>)<sub>3</sub>-catalyzed group transfer polymerization of alkyl methacrylates with dimethylphenylsilane through in situ formation of silyl ketene acetal by B(C<sub>6</sub>F<sub>5</sub>)<sub>3</sub>-catalyzed 1,4-hydrosilylation of methacrylate monomer. *Polym. Chem.* **2015**, *6*, 3502–3511. [[CrossRef](#)]
63. Xu, T.; Chen, E.Y.-X. Silylium dual catalysis in living polymerization of methacrylates via in situ hydrosilylation of monomer. *J. Polym. Sci. A Polym. Chem.* **2015**, *53*, 1895–1903. [[CrossRef](#)]
64. Li, J.; Mizutani, S.; Sato, S.; Narumi, A.; Haba, O.; Kawaguchi, S.; Kawaguchi, S.; Kakuchi, T.; Shen, X. Thermoresponsive property of well-defined poly(N-methyl-N-n-propylacrylamide) and its copolymer architectures prepared by hydrosilylation-promoted group transfer polymerization. *Polymer* **2020**, 122678. [[CrossRef](#)]
65. Hidaka, T.; Sugihara, S.; Maeda, Y. Infrared spectroscopic study on LCST behavior of poly(N,N-bis(2-methoxyethyl)acrylamide). *Eur. Polym. J.* **2013**, *49*, 675–681. [[CrossRef](#)]
66. Song, J.M.; Winnik, F.M.; Brash, J.L. Synthesis and Solution Properties of Fluorescently Labeled Amphiphilic (N-alkylacrylamide) Oligomers. *Macromolecules* **1998**, *31*, 109–115. [[CrossRef](#)]
67. Koyama, M.; Hirano, T.; Ohno, K.; Katsumoto, Y. Molecular Understanding of the UCST-Type Phase Separation Behavior of a Stereocontrolled Poly(N-isopropylacrylamide) in Bis(2-methoxyethyl) Ether. *J. Phys. Chem. B* **2008**, *112*, 10854–10860. [[CrossRef](#)]
68. Yamazaki, A.; Winnik, F.M.; Cornelius, R.M.; Brash, J.L. Modification of liposomes with N-substituted polyacrylamides: Identification of proteins adsorbed from plasma. *Biochim. Biophys. Acta Biomembr.* **1999**, *1421*, 103–115. [[CrossRef](#)]
69. Hechenbichler, M.; Laschewsky, A.; Gradzielski, M. Poly(N,N-bis(2-methoxyethyl)acrylamide), a thermoresponsive non-ionic polymer combining the amide and the ethyleneglycolether motifs. *Colloid Polym. Sci.* **2020**, *299*, 205–219. [[CrossRef](#)]
70. El-Ejmi, S.; Huglin, B. Thermoreversible behaviour in water of chemically crosslinked poly(2-methoxyethylacrylate-co-N,N-dimethylacrylamide). *Polym. Int.* **1997**, *44*, 277–282. [[CrossRef](#)]
71. Fu, X.; Wang, Y.; Xu, L.; Narumi, A.; Sato, S.; Yang, X.; Shen, X.; Kakuchi, T. Thermoresponsive Property of Poly(N,N-bis(2-methoxyethyl)acrylamide) and Its Multiblock Copolymers with Poly(N,N-dimethylacrylamide) Prepared by Hydrosilylation-Promoted Group Transfer Polymerization. *Polym. Chem.* **2023**, *14*, 5060–5070. [[CrossRef](#)]
72. Kikuchi, S.; Chen, Y.; Kitano, K.; Takada, K.; Satoh, T.; Kakuchi, T. Organic acids as efficient catalysts for group transfer polymerization of N,N-disubstituted acrylamide with silyl ketene acetal: Polymerization mechanism and synthesis of diblock copolymers. *Polym. Chem.* **2015**, *6*, 6845–6856. [[CrossRef](#)]

**Disclaimer/Publisher’s Note:** The statements, opinions and data contained in all publications are solely those of the individual author(s) and contributor(s) and not of MDPI and/or the editor(s). MDPI and/or the editor(s) disclaim responsibility for any injury to people or property resulting from any ideas, methods, instructions or products referred to in the content.